Semiconductive and redox properties of Ti and Zr pyrophosphate catalysts (TiP_2O_7 and ZrP_2O_7). Consequences for the oxidative dehydrogenation of *n*-butane

Ioan-Cezar Marcu [a], Jean-Marc M. Millet [a]*, and Jean-Marie Herrmann [b]

[a] *Institut de Recherches sur la Catalyse, CNRS, associé à l'Université Claude Bernard Lyon I, 2 avenue A. Einstein, F-69626 Villeurbanne Cedex, France*

[b] *Laboratoire de Photocatalyse, Catalyse et Environnement, (LPCE), UMR CNRS 5621, Ecole Centrale de Lyon, BP 163, 69131, Ecully Cedex, France*

Received 9 August 2001; accepted 26 October 2001

The electrical conductivity of titanium and zirconium pyrophosphates used as catalysts in *n*-butane oxidative dehydrogenation has been measured under oxygen and *n*-butane at 400 and 500 °C and under subsequent exposures to both gases at the catalytic reaction temperature. The two compounds appeared to be p-type semiconductors under air with positive holes as the main charge carriers but became n-type when contacted with *n*-butane. If their conductivities are comparable as p-type semiconductors (within one order of magnitude), by contrast, they differ by 3 orders of magnitude when being n-type semiconductors. These results explain the difference in catalytic reaction mechanism encountered on the two solids. The alkane activation was proposed to be related in both cases to the p-type semiconducting properties of the solids, likely through hydrogen abstraction by a surface O^- species, forming a $C_4H_9^{\bullet}$ radical which will similarly undergo a second hydrogen abstraction to form butenes. The changes in activation energy and in selectivity on TiP_2O_7 at higher temperatures (>450 °C) are indicative of a change in mechanism, possibly with the transient formation of an alkoxide species.

KEY WORDS: TiP_2O_7 and ZrP_2O_7 catalysts; dehydrogenation of *n*-butane

1. Introduction

Electrical conductivity measurements carried out on oxide-based catalysts can provide information on the nature of surface structure defects, the existence of oxidizing species (ionosorbed oxygen species, active surface anions, etc.) and the nature of the oxidic phase involved in catalytic reactions as described in ref. [1]. This is particularly true for the catalysts used in oxidation reactions based on redox processes between reactants and catalysts. The electrical behavior of these catalysts is generally a function (i) of the temperature, whose influence can be followed in the same range as that of catalysis; (ii) of the oxygen pressure; and (iii) of the nature of the gas phase in contact with the solid. DC-electrical conductivity measurements constitute a useful tool to investigate such gas–solid electronic interactions. Electrical conductivity measurements appear as a choice method to characterize oxidation catalysts. Consequently, this technique was applied to tetravalent metal pyrophosphates, such as TiP_2O_7 and ZrP_2O_7, used in the oxidative dehydrogenation of *n*-butane.

To our knowledge, none of the electrical and catalytic properties of these solids has been yet reported. In the present study DC-electrical conductivity of TiP_2O_7 and ZrP_2O_7 was studied as a function of (i) temperature; (ii) air and pure oxygen pressure; (iii) the nature of the pure gaseous reactant atmospheres (oxygen or *n*-butane); (iv) the reaction mixture; and (v) the crystallinity of TiP_2O_7. A comparison between both pyrophosphate catalysts and between two types of homemade TiP_2O_7 solids, one crystallized and the other amorphous, has also been established.

* To whom correspondence should be addressed.

2. Experimental

2.1. Catalyst preparation and characterization

Two methods have been used to prepare the pyrophosphate catalysts. The first one (A) was based on the reaction of phosphoric acid (85%) with the corresponding metal oxide [2]. The homogeneous slurry formed was dried and calcined at 120 and 700 °C for TiP_2O_7 and at 200, 400 and 900 °C for ZrP_2O_7.

The second method (B), based upon a sol-gel method, has been used for the preparation of one TiP_2O_7 sample only. A titanium di-isopropoxide *bis*(2,4-pentanedionate) solution in isopropanol was hydrolysed with an aqueous solution of 0.3 M H_3PO_4 at a pH maintained at 9 by addition of an ammonia solution. The resulting gel was recovered by centrifugation and repeatedly washed with distilled water, then dried in air at 60 °C and eventually calcined at 650 °C.

The crystal structure of the compounds was controlled by X-ray diffraction. The solids prepared using method A

1011-372X/02/0300-0273/0

corresponded to well crystallized pure phases whereas those prepared using method B were amorphous. The BET surface areas of the TiP_2O_7-A, ZrP_2O_7 and TiP_2O_7-B samples were equal to 6, 1.5 and $3\,m^2\,g^{-1}$, respectively.

UV spectra were recorded with a Perkin–Elmer Lambda-9 spectrophotometer from 200 to 500 nm with a diffuse reflectance attachment using MgO as a reference.

2.2. Catalytic test

The oxidative dehydrogenation of *n*-butane was performed in a fixed-bed quartz tube down-flow reactor operating at atmospheric pressure. The apparatus and the conditions have been described elsewhere [2]. A gas feed ($air/C_4H_{10} = 5/1$) was used at 530 °C with a VVH of $1000\,h^{-1}$ with respect to *n*-butane. The major products formed under these reaction conditions were 1- and 2-butenes, butadiene, CO, CO_2, and cracking products (methane, ethane, ethene and propene).

2.3. Electrical conductivity measurements

A general description of the static cell used for the electrical conductivity measurements has been reported previously [1]. Samples of Ti or Zr pyrophosphate catalyst (*ca.* 200 mg) were slightly compressed (*ca.* 1×10^5 Pa) between two platinum electrodes to ensure good electrical contacts between the grains without modifying the texture or preventing gas–solid interactions on the surface of the solid. The temperature was controlled using thermocouples soldered to the electrodes and, when short-circuited, they were used to determine the electrical conductivity σ of the samples, which can be expressed by the formula

$$\sigma = \frac{1}{R} \times \frac{t}{S} \qquad (1)$$

where R is the electrical resistance and t/S is the geometrical factor including the thickness t (*ca.* 2.5 mm) and the cross-sectional area S of the circular electrodes whose diameter is equal to 1.00 cm. The electrical resistance was measured with an ohmmeter (Kontron, Model DMM 4021) for $1 \leqslant R \leqslant 2 \times 10^6$ ohms and with a teraohmmeter (Guildline Instruments Model 9520) for $10^6 \leqslant R \leqslant 10^{14}$ ohms.

To compare the electrical conductivities of the pyrophosphate samples, it is required that the solids have similar textures and identical surface states. This requirement is easily fulfilled since all the samples have similar textures. Indeed, the electrical conductivity of an n-type semiconductor powder can be written as

$$\sigma = A[e^-] \qquad (2)$$

where $[e^-]$ is the concentration of quasi-free electrons and A is a textural parameter depending on the compression of the powder and on the number and quality of contact points between particles [1]. Since all the samples have similar BET surface areas and since electrical measurements were standardized, A can be considered as identical for all the samples under identical conditions.

The common reference state for σ determination has been chosen under air at atmospheric pressure and at 500 °C. At this temperature, which is close to that used in the catalytic reactions, most of the ionically adsorbed species such as H_3O^+ and HO^- which would produce an additional surface conductivity are eliminated. The solid was initially heated from room temperature to 500 °C at a heating rate of 5 °C/min.

3. Results

3.1. Catalytic performances of the pyrophosphate catalysts

Although the present work is devoted to the electrical and redox properties of these solids, it is important to describe their catalytic performances in *n*-butane oxidative dehydrogenation (ODH) reaction.

The pyrophosphates presented very different activities but were all selective towards oxidative dehydrogenation products (table 1). Zirconium pyrophosphate appeared

Table 1
Catalytic performances of the pyrophosphate catalysts at 530 °C

Catalyst	Conv. (%)	Selectivities (%)					$\frac{1-C_4'}{2-C_4}$ [f]	v_i [g] ($10^8\,mol\,s^{-1}\,m^{-2}$)
		C_4' [a]	C_4'' [b]	TDS[c]	CRA[d]	CO_x [e]		
ZrP_2O_7	12	59	2	61	35	4	1.5	109
TiP_2O_7-A	25	42	14	56	22	22	0.5	60
TiP_2O_7-B	5	34	4	38	27	35	0.4	47

[a] Butenes.
[b] Butadiene.
[c] Total dehydrogenation selectivity.
[d] Cracking products.
[e] CO and CO_2.
[f] 1-Butene/2-butenes molar ratio.
[g] Intrinsic activity for the conversion of *n*-butane.

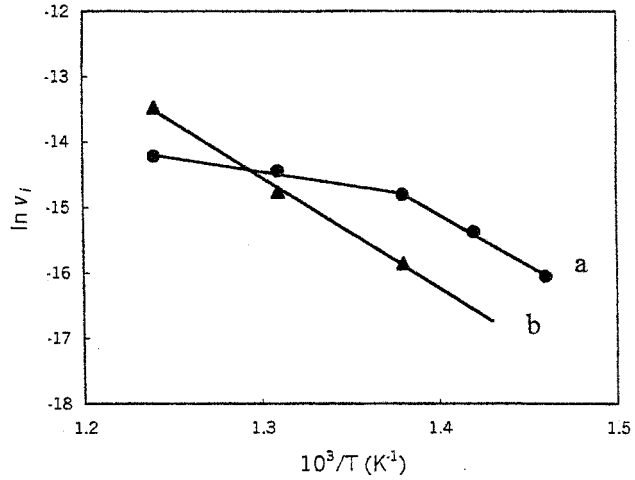

Figure 1. Arrhenius plots for the *n*-butane conversion on TiP_2O_7-A (a) and ZrP_2O_7 (b).

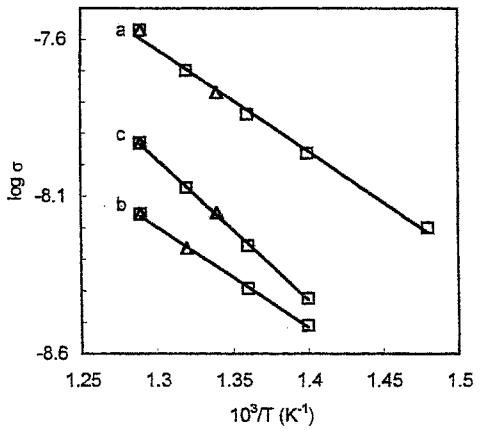

Figure 2. Arrhenius plots for the electrical conductivity σ of TiP_2O_7-A (a); ZrP_2O_7 (b); and TiP_2O_7-B (c) (□—decreasing temperatures; △—increasing temperatures; under air at atmospheric pressure; σ in ohm^{-1} cm^{-1}.)

as the most active catalyst but titanium pyrophosphate led to the best yields in butenes and butadiene. The main difference concerned the product distribution: TiP_2O_7 oxidized mainly *n*-butane to butadiene and carbon oxides, whereas on ZrP_2O_7 the reaction was limited to the formation of butenes. In the latter case, the 1-butene/2-butenes ratio was equal to 1.5 instead of the equilibrium ratio of 0.5 obtained on TiP_2O_7. TiP_2O_7-B gave a conversion five times lower than that of TiP_2O_7-A and the selectivity in CO_x increased at the expense of the total dehydrogenation selectivity (TDS).

The activation energies corresponding to the transformation of *n*-butane on the crystallized catalysts have been calculated. The Arrhenius plots obtained are presented in figure 1. The activation energies on ZrP_2O_7 and TiP_2O_7-A at low temperature were close to each other (140 and 129 kJ mol^{-1} respectively), whereas that found on TiP_2O_7-A at high temperature was very different (35 kJ mol^{-1}). Such results are consistent with the existence of two different reaction mechanisms for the activation of *n*-butane on TiP_2O_7, with a transition occurring at *ca.* 450 °C according to figure 1.

3.2. Electrical conductivity measurements

(a) Variations of the electrical conductivity as a function of temperature

The electrical conductivities of the pyrophosphates have been measured as a function of temperature to determine the activation energy of conduction E_c under air at atmospheric pressure. To ensure the reversibility of the experiments, the measurements were performed with increasing and decreasing temperature. The semi-log plots [$\log\sigma = f(1/T)$] obtained are given in figure 2. The slopes enabled one to calculate the E_c values: 62.2 and 61.8 kJ mol^{-1} (0.65 eV) for TiP_2O_7-A and ZrP_2O_7, respectively. It can be observed that the two solids have identical values for E_c. In the case of TiP_2O_7-B, the E_c value calculated from the slope of the line is equal to 86.5 kJ mol^{-1} (0.9 eV). It can be observed that this value is substantially greater by 24 kJ mol^{-1} (0.25 eV) than that corresponding to TiP_2O_7-A.

(b) Variations of the electrical conductivity as a function of air and oxygen pressure

The electrical conductivity σ of TiP_2O_7-A and ZrP_2O_7 catalysts was measured as a function of oxygen pressure under air and under pure oxygen. In all cases it was observed that the conductivity varied linearly with the air pressure (figure 3). Moreover, they are all of the p-type under air atmosphere since $\partial\sigma/\partial P_{O_2} > 0$.

As the aim of the present work is to characterize the semiconductive properties of catalysts, it is relevant to first briefly summarize the theoretical aspect of p-type semiconductivity.

σ varies with T and P_{O_2} according to the general equation

$$\sigma = \sigma_0 \exp(-E_c/RT) P_{O_2}^{+1/n}. \quad (3)$$

Depending upon the value of n, the mode of conduction can be related to a special type of structure defects acting as hole sources.

It has been shown [1] that, for a transition metal oxide MO, a conduction model with $n = 4$ corresponds to singly ionised cationic vacancies whose formation involves the following equilibria:

$$\tfrac{1}{2}O_{2(g)} \overset{K_4}{\rightleftharpoons} O^{2-} + V_{M^{2+}} \quad (4)$$

$$V_{M^{2+}} \overset{K_5}{\rightleftharpoons} V^{-}_{M^{2+}} + p^{+} \quad (5)$$

where $V_{M^{2+}}$ and $V^{-}_{M^{2+}}$ represent cationic vacancies with respectively two and one positive charges localised around the defect.

However, in the present case, Ti^{4+} and Zr^{4+} are tetravalent cations and the model relative to MO oxides cannot be applied. The initial p-type character of

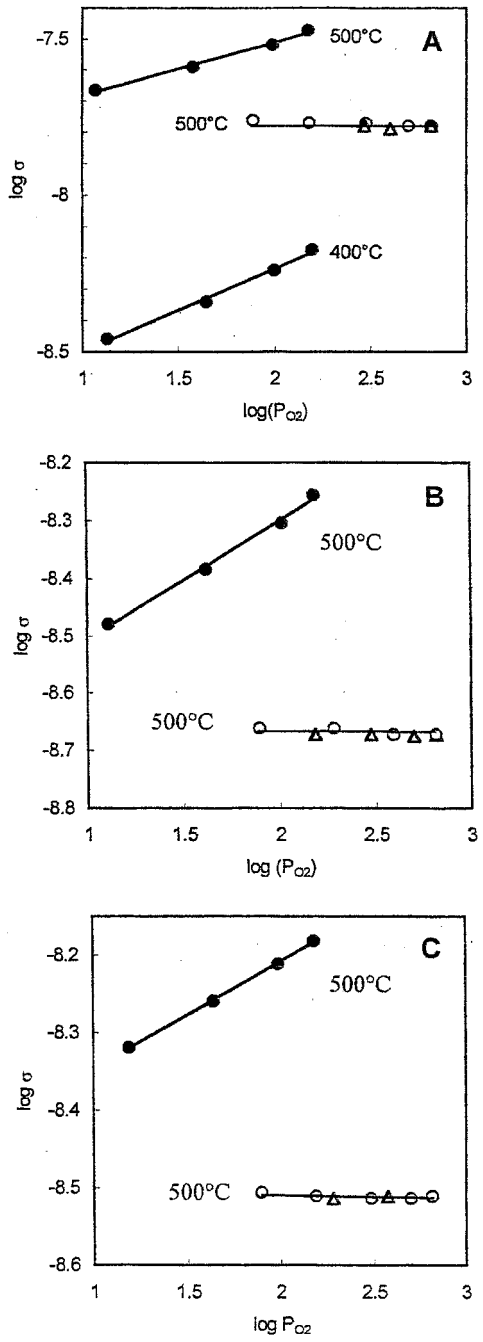

Figure 3. log–log plot of the variations of σ as function of the oxygen pressure for TiP_2O_7-A (A); ZrP_2O_7 (B); and TiP_2O_7-B (C) (●—under air; ○—under increasing oxygen pressure; △—under decreasing oxygen pressure; P_{O_2} in Torr; σ in ohm^{-1} cm^{-1}.)

TiP_2O_7 and ZrP_2O_7 can be accounted for by a chemisorption model of oxygen associated with the formation of holes p^+ according to the equilibrium:

$$\tfrac{1}{2}O_{2(g)} \overset{K_6}{\rightleftharpoons} O^- + p^+. \tag{6}$$

The mass action law applied to equation (6) gives:

$$K_6 = [O^-][p^+]/P_{O_2}^{1/2} \tag{7}$$

and the electroneutrality condition implies:

$$[O^-] = [p^+]. \tag{8}$$

The combination of equations (7) and (8) yields:

$$\sigma \propto [p^+] = K_6^{1/2} P_{O_2}^{1/4}. \tag{9}$$

Actually, the log–log plots of σ as a function of P_{O_2} in air give ascending straight lines whose slopes are close to $+1/4$ (figure 3). This indicates that all solids behave similarly with respect to oxygen pressure in air. In addition, the constant K_6 follows van't Hoff's law as a function of temperature:

$$K_6 = (K_6)_0 \exp(-\Delta H_6/RT) \tag{10}$$

ΔH_6 being the enthalpy of reaction (6).

Combining equations (9) and (10), one gets:

$$\sigma \propto [p^+] = [(K_6)_0]^{1/2} \exp(-\Delta H_6/2RT) P_{O_2}^{1/4}. \tag{11}$$

Since the solids are semiconductors, *i.e.*, having a conductivity varying exponentially with temperature according to equation (3), as illustrated by figure 2, there results from equations (3) and (11), the identity:

$$\Delta H_6 = 2E_c. \tag{12}$$

Since E_c is the same for both TiP_2O_7 and ZrP_2O_7 pyrophosphates (62 kJ mol^{-1}), this means that oxygen ionosorption creates identical O^- species with an enthalpy of formation ΔH_6 equal to:

$$\Delta H_6 = 2E_c = 124\,\text{kJ mol}^{-1}.$$

When air was replaced by pure oxygen, the electrical conductivity became almost independent of the oxygen pressure (figure 3). This could lead to the conclusion that all three compounds have become intrinsic semiconductors ($\partial\sigma/\partial P_{O_2} = 0$). If that were the case, the theory would imply that the band-gap energy E_G should be equal to twice the activation energy of conduction E_c ($E_G = 2E_c$). Consequently, E_G should be equal to 1.3 eV for both TiP_2O_7-A and ZrP_2O_7 and to 1.8 eV for TiP_2O_7-B. However, the band-gap energies determined from the UV spectra in figure 4 are equal to 3.8, 5.1 and 3.5 eV, respectively. These values are quite different from those calculated, and the solids cannot be considered as intrinsic semiconductors under our conditions but as extrinsic ones with sources of electrical charge carriers independent of oxygen pressure.

(c) *In situ* electrical conductivity measurements under catalytic conditions

To get information on the solids under conditions as close as possible to those of catalysis, the electrical conductivity measurements were performed at reaction temperature during sequential periods under *n*-butane, then under

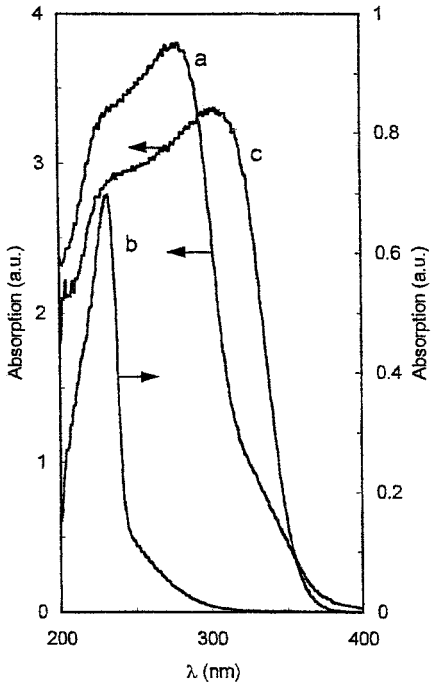

Figure 4. UV-visible absorption spectra of TiP_2O_7-A (a) (band gap: 3.9 eV), ZrP_2O_7 (b) (band gap: 5.8 eV) and TiP_2O_7-B (c) (band gap: 3.5 eV).

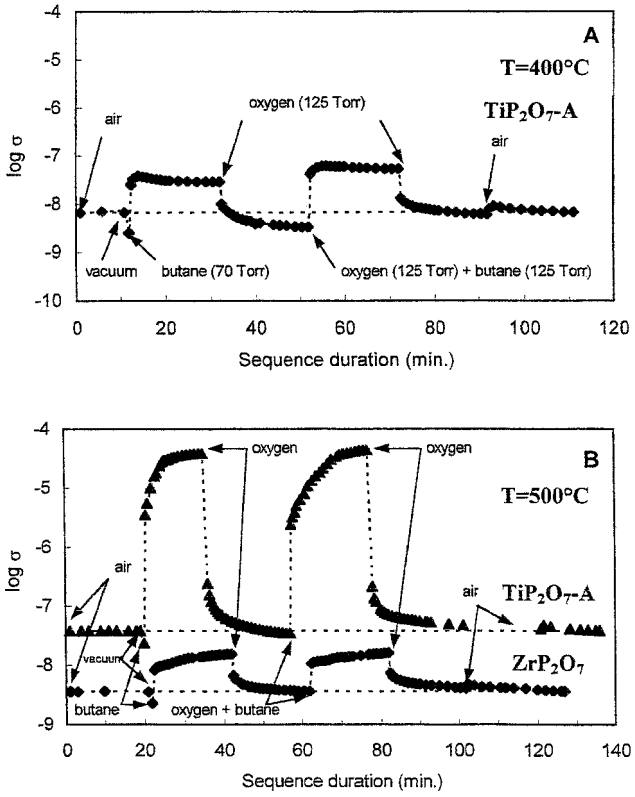

Figure 5. Variations of the electrical conductivity under sequential exposures to *n*-butane (70 Torr), to oxygen (125 Torr) and under *n*-butane (125 Torr)–oxygen (125 Torr) mixture for TiP_2O_7-A at 400 °C (A) and for ZrP_2O_7 (◆) and TiP_2O_7-A (▲) at 500 °C (B).

oxygen and eventually under an *n*-butane–oxygen reaction mixture, with oxygen and *n*-butane partial pressures equal to those of the reaction feeds used in the catalytic tests (*n*-butane: 125 Torr, oxygen: 125 Torr).

After heating the solids from room temperature to 500 or to 400 °C, at a heating rate of 5 °C/min in air at atmospheric pressure, and after outgassing in air within less than half a minute, *n*-butane was introduced in contact with the samples. In the case of TiP_2O_7-A catalyst at 500 °C, the electrical conductivity immediately increased abruptly by 3 orders of magnitude (figure 5(B)). When the temperature was equal to 400 °C, the electrical conductivity increased by only 1 order of magnitude (figure 5(A)). The same variations of the electrical conductivity were observed for ZrP_2O_7 catalyst at 500 °C, but within less than 1 order of magnitude. These behaviors are typically those of n-type semiconductors.

After reaching the steady state under *n*-butane, the gas phase was promptly evacuated and replaced by pure oxygen. The electrical conductivity of TiP_2O_7-A and ZrP_2O_7 decreased immediately and reached a plateau (figure 5), either at 400 or 500 °C. This behavior confirmed the n-type character of the two pyrophosphates, since, for oxide semiconductors, the n-type criterion is $\partial\sigma/\partial P_{O_2} < 0$. The solids behave as redox relays according to the nature of the gas phase in contact.

During successive sequences in *n*-butane and oxygen, TiP_2O_7-B at 500 °C had the same behavior as TiP_2O_7-A (figure 6), but the electrical conductivity varied within *ca.* 1 order of magnitude in the first case in comparison with 3 orders of magnitude in the second one.

It is interesting to note that the introduction of *n*-butane in contact with the solid changed the nature of the semiconductivity of all solids, passing from p-type in air to n-type conduction, since $\partial\sigma/\partial P_{C_4H_{10}} > 0$. Such a phenomenon of σ can be ascribed to new sources of electrons. Free electrons can arise from the creation of

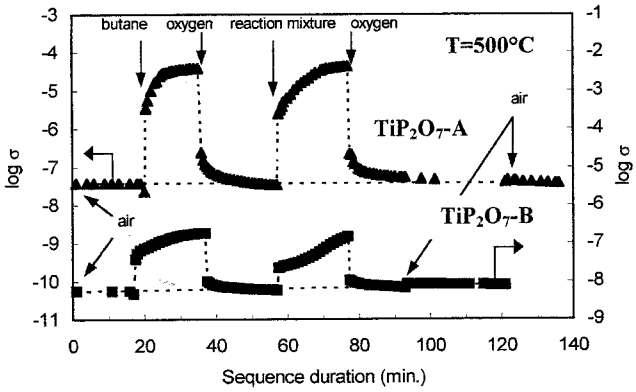

Figure 6. Variations of the electrical conductivity under sequential exposures to *n*-butane (70 Torr), oxygen (125 Torr) and an *n*-butane–oxygen mixture (125 Torr–125 Torr) for TiP_2O_7-A (▲) and TiP_2O_7-B (■) at 500 °C.

anionic vacancies, V_O, by reduction of the solid by *n*-butane:

$$(O^{2-})^0 + C_4H_{10} \rightarrow C_4H_8 + H_2O + V_O \qquad (13)$$

or by butenes, which are intermediates of reaction in the case of TiP_2O_7:

$$(O^{2-})^0 + C_4H_8 \rightarrow C_4H_6 + H_2O + V_O \qquad (14)$$

followed by the ionisation of the anionic vacancy:

$$V_O \overset{K_{15}}{\rightleftharpoons} V_O^+ + e^- \qquad (15)$$

$$V_O^+ \overset{K_{16}}{\rightleftharpoons} V_O^{2+} + e^-. \qquad (16)$$

$(O^{2-})^0$ represents an oxygen anion of the solid. The zero-charge superscript indicates that it is a neutral entity with respect to the solid. V_O represents a filled anionic vacancy and V_O^{2+} a doubly ionized anionic vacancy.

The second possible source of quasi-free electrons in pyrophosphates can originate from the consumption of negatively charged species at the surface, such as O^-:

$$C_4H_{10} + O^- \rightarrow C_4H_8 + H_2O + e^-. \qquad (17)$$

After the measurement under pure oxygen, O_2 was promptly evacuated and the catalytic reaction mixture (125 Torr of *n*-butane and 125 Torr of oxygen) was introduced in contact with the solid. Instantaneously, the electrical conductivity increased because of the reducing nature of *n*-butane (equations (13) and (15)) and reached a plateau (figures 5 and 6). In all cases, the electrical behavior of the pyrophosphate catalysts indicated that they were n-type semiconductors under catalytic reaction conditions as they were under pure *n*-butane.

4. Discussion

The aim of this work was to better characterize Zr and Ti pyrophosphate catalysts used for the oxidative dehydrogenation of *n*-butane and to simultaneously gain information on their redox properties with respect to *n*-butane.

We have seen that Zr and Ti pyrophosphates were p-type semiconductors under air but became n-type semiconductors when contacted with *n*-butane.

A p-type semiconductor can be characterized either by an excess of anionic oxygen or by cationic vacancies.

If we consider that the O^- anions correspond to the "chemical site" of a hole [3], according to the reaction

$$O^{2-} + p^+ \rightarrow O^- \qquad (18)$$

and that the nature of semiconductivity changes from p to n when *n*-butane is contacted with the solid, we consider that in the case of ZrP_2O_7 only the mechanism involving the consumption of negatively charged species O^- at the surface is involved according to equation (17), whereas in the case of TiP_2O_7, the consumption of the negatively charged species O^- at the surface of solid by the *n*-butane and a reduction of the catalyst according to equations (13) or (14) should simultaneously be involved. The first mechanism would be dominant at 400 °C.

At lower temperatures the initial step of the alkane activation is similar on both solids since the activation energies of the reaction are equal (figure 1). It may take place *via* the attack of the hydrocarbon at a positive hole site (p-type semiconductivity) leading to a hydrocarbon radical, as proposed earlier [3]:

$$C_4H_{10} + O^- \rightarrow C_4H_9^{\bullet} + O^{2-} + H^+. \qquad (19)$$

The radical formed would rapidly undergo a second hydrogen abstraction according to a similar mechanism leading to butene:

$$C_4H_9^{\bullet} + O^- \rightarrow C_4H_8 + O^{2-} + H^+ \qquad (20)$$

$$O^{2-} + 2H^+ \rightarrow H_2O_{(g)}. \qquad (21)$$

At higher temperatures, the reaction mechanism remains unchanged on ZrP_2O_7. By contrast, TiP_2O_7 exhibits a change in the mechanism illustrated by a substantially lower activation energy (35 *versus* 129 kJ mol^{-1}). Correspondingly, it can be noted that the selectivities in butadiene and in CO_x are increased and the 1-butene/2-butenes ratio decreased from 1.5 to the thermodynamic equilibrium value of 0.5 (table 1). The change in mechanism could be ascribed to the transient formation of an alcoxide intermediate, already mentioned in ref. [4]. It seems that the formation of this intermediate implies an anionic vacancy.

Such a mechanism, which has already been proposed for propane activation on vanadium antimonate [5], leads to a more stable intermediate that could be further dehydrogenated to butadiene. This higher stability would explain the difference in 1-butene/2-butenes ratios encountered on TiP_2O_7 and the negative role of water [2].

The comparison of TiP_2O_7-A and TiP_2O_7-B indicates that the electrical conductivity σ depends on the crystallinity of the solid: in the case of TiP_2O_7-B which is amorphous, σ is approximately 3 orders of magnitude lower. Furthermore, it has been observed that the electrical conductivity increases more abruptly on the amorphous TiP_2O_7-B and ZrP_2O_7 rather than on crystallized TiP_2O_7-A. This can be explained by the fact that not only a surface phenomenon, *i.e.*, the formation of surface anionic vacancies, occurs but also a bulk phenomenon, *i.e.*, the diffusion of oxygen vacancies into the volume. This observation confirms the importance of anionic vacancies in the mechanism on TiP_2O_7

which can be ascribed to a Mars and van Krevelen type mechanism [6].

References

[1] J.-M. Herrmann, in: *Catalyst Characterization*, *Physical Techniques for Solid Materials*, eds. B. Imelik and J.C. Védrine (Plenum Press, New York, 1994) ch. 20.

[2] I.C. Marcu, I. Sandulescu and J.M.M. Millet, Appl. Catal. A, submitted for publication.

[3] J.-M. Herrmann, P. Vernoux, K.E. Béré and M. Abon, J. Catal. 167 (1997) 106.

[4] H.H. Kung, Adv. Catal. 40 (1994) 1.

[5] H. Roussel, B. Mehlomakulu, F. Belhadj, E. van Steen and J.M.M. Millet, J. Catal. to be published.

[6] S. Mars and N. van Krevelen, Chem. Eng. Sci., Special Sup. 9 (1954) 41.